J Theor Appl Phys (2015) 9:135–140
DOI 10.1007/s40094-015-0171-y

RESEARCH

Glass surface modification using Nd:YAG laser in SF_6 atmospheres

H. R. Dehghanpour · P. Parvin

Received: 2 September 2014 / Accepted: 7 February 2015 / Published online: 27 February 2015

Abstract Glass surface modification is one of the processes which changes its physical properties. Changing optical property is a significant effect of surface modification. Among the surface modification methods, laser surface modification is attractive for researchers. Here, SiO_2 glass target was irradiated by Q-switched Nd:YAG laser (1064 nm) in SF_6 atmospheres as well as vacuum. In this process, an Nd:YAG laser beam was focused near the glass target while the target was inserted in a chamber containing SF_6 atmosphere or at vacuum condition. The surface morphology changes were investigated by scanning electron microscopy (SEM). Noticeable surface changes were observed due to laser irradiation in SF_6 atmosphere. Although the absorption lines of SF_6 molecule are not near the Nd:YAG laser wavelength, laser-induced breakdown spectroscopy (LIBS) showed decomposition of SF_6 molecules near a glass target. The ablated fragments from the target impacted on gas molecules and decomposed them. In this work, LIBS showed that there were several fluorine ions when the target was irradiated in an SF_6 atmosphere. This demonstrates SF_6 molecule decomposition near the glass target by laser irradiation. The plasma temperature was $\sim$2000 K. This temperature is much less than metallic or other gaseous materials' plasma temperatures.

Keywords Surface modification · SF_6 decomposition · Fluorine penetration · Glass · Laser

H. R. Dehghanpour (✉)
Physics Department, Tafresh University, Tafresh, Iran
e-mail: h.dehghanpour@aut.ac.ir

P. Parvin
Physics Department, Amirkabir University of Technology, Tehran, Iran

Introduction

By increasing glass microdevices' applications, the necessary, low-priced, simple and flexible microstructuring techniques have vastly increased. Making precise surface microstructuring of the materials to fabricate highly integrated microdevices is one of the essential technologies of photonics. Moreover, UV-transparent materials such as amorphous SiO_2 glass, quartz, MgF_2, CaF_2 and LiF are important materials for optical device fabrication. Microfabrication of SiO_2 glass as a hard and brittle optical material is difficult. In practice, surface microstructures on glass are created by approaches based on photoresistant protection layer coating, lithography, etching and cleaning steps. Finding new techniques to decrease the time-consuming stages of the microfabrication is necessary [1].

An efficient and popular technique with attractive applications in many areas is laser-induced breakdown spectroscopy (LIBS). The main advantages of LIBS are: multi-elemental capability, low cost, the simplicity of working in wide range pressure environments and detection of various components in a great variety of matrices.

In LIBS, at first the pulsed laser is focused on the target. For the nanosecond pulses the energies are in the GW cm^{-2} range, which is high enough for plasma creation through the vaporization, atomization and ionization processes in a single setup. A high-temperature dense plasma is the result of the process which could be spectrally resolved and detected. It contains the characteristic peaks with significant information on the nature and concentration of the elements. The number density of the corresponding emitting species in the plume is proportional to integrated emission of the individual spectral lines.

Pulsed laser irradiation on the SiO_2 surface in an SF_6 atmosphere induces gas decomposition [2]. It produces

reactive species to restructure the glass surface too. The irradiations on amorphous SiO_2 glass were performed at different wavelengths [1–3]. During Nd:YAG laser irradiation, the possibility for energy absorption by free electrons via the inverse Bremsstrahlung (IB) process leads to increase in the electron–molecule collision rate and the generation of weak plasma. It rarely creates molecular formation in accordance with a larger amount of fluorine trace in the solid [1]. Furthermore, fluorine penetration in the silicon content under plasma treatment and the diffusion of ion implanted-F in Si have been previously studied by various spectroscopic techniques [4]. Though theoretical studies emphasize that F diffusion involves normal interstitial motion in the perfect Si crystal, anomalous diffusion causes the depletion of F to only occur at temperatures above 550 °C, suggesting a thermally activated process which is strongly temperature dependent. Direct observation of volatile Si oxy-fluoride and Si fluoride moieties between F and SiO_2 (or Si) precede desorption of F from Si. The driving force for the observed anomalous F migration remains unknown [4]. In this work, we investigate surface modification on the glass surface by Q-switched Nd:YAG laser at different atmospheres. Furthermore, using LIBS the SF_6 decomposition near the glass target as well as the temperature of the irradiated glass surface were calculated.

Experimental apparatus

The experimental setup consists of a stainless steel irradiation chamber, $\sim$100 cm^3, with cross-type quartet windows, high vacuum-mixing system, Q-switched Nd:YAG laser (1064 nm, 150 mJ/pulse, 10 ns duration, 1–20 Hz) and conducting and focusing optics as shown in Fig. 1. An AR-coated MgF_2 window and a glass slab were inserted opposite to each other as coupler and target. A semiconductor detector (PIN, EG&G, FNT100), a Tektronix 7844 400 MHz oscilloscope and a Coherent™ J m (Field Master, LM-P10 and LM-P5 LP heads) were used for the relative and absolute power measurements. The laser energy delivered to the cell was varied using several NDF aluminized attenuators with the appropriate optical densities. LIBS arrangement consists of a CCD-coupled transmission grating spectrometer and the corresponding optics and data processing. The light emission of plasma was collected by a fiber bundle (UV 600/660 type with SMA-905 fiber connector and 1 m length) using a quartz lens (25 mm diameter, 50 mm focal length) placed 80 mm away from the sample. The fiber output was coupled to the entrance slit of the compact wide range spectrometer (200–1100 nm) model S150 Solar laser system (50 mm focal length, transmission diffraction grating with 200 Grooves/mm with 0.02 × 3.0 mm of entrance slit and 0.5 nm spectral resolutions). A charged coupled device (CCD) detector array model Toshiba TCD1304AP with 3648 pixels was used to detect the dispersed light subsequently. The CCD camera was triggered $\sim$2 μs after the onset of the laser shot using a suitable delay generator to reduce the continuum Bremsstrahlung radiation. The LIBS setup is shown in Fig. 2.

Experiments

The experiments were done using different cell content SF_6 gas at 800 mbar pressure as well as vacuum to investigate the surface morphology modification due to laser irradiation. At first, LIBS of amorphous SiO_2 glass in SF_6 atmosphere (800 mbar) was performed using a focused Nd:YAG laser beam at 1064 nm. Then, the surface morphology of the treated surfaces was studied. SEM micrographs of irradiated surfaces in the vacuum and chamber filled with SF_6 were obtained.

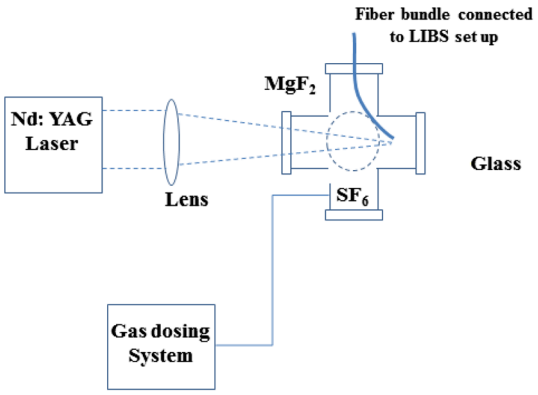

Fig. 1 Experimental arrangement for the laser irradiation of amorphous SiO_2 glass

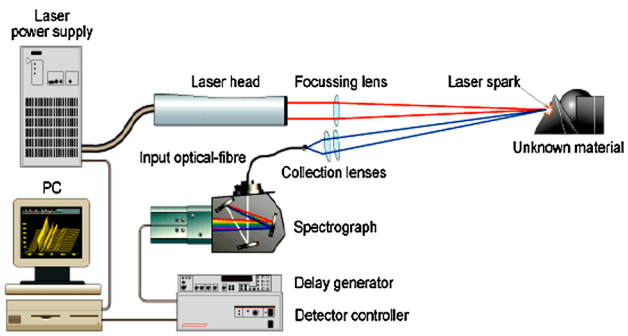

Fig. 2 A schematic of the LIBS setup

Theory

LIBS

The energy level population of the plasma species is proportional to the intensity of plasma's spectral line emission. Local thermodynamic equilibrium (LTE) and being optically thin are the basic assumptions about the plasma. The LTE condition is given by the relation [5]:

$$N_e \geq 1.6 \times 10^{12} T^{1/2} \Delta E^3, \quad (1)$$

where N_e is the electron density, $T(K)$ shows the plasma temperature and ΔE (eV) denotes the largest energy transition for which the condition holds. Electron density is known as an important plasma parameter that gives indications about the thermal equilibrium. The experimental condition satisfies the LTE condition and as a result Eq. 1 is valid. So, the Boltzmann equation is used to express the population of an excited level based on the number density ns of the species within the plasma [5]:

$$I_{ij} = \frac{A_{ij} g_i}{U_S(T)} n_S \exp\left(-\frac{E_i}{kT_e}\right), \quad (2)$$

where A_{ij}, E_i, g_i, k and U_S are the transition probability, the excitation energy of the level, the statistical weight for the upper level, the Boltzmann constant and the partition function of the species at electronic temperature T_e, respectively. Therefore, the plasma temperature is determined according to the Boltzmann plot:

$$\ln\left(\frac{I_{ij}}{A_{ij} g_i}\right) = \ln\left(\frac{n_S}{U_S(T)}\right) - \frac{E_i}{kT_e}. \quad (3)$$

Fluences higher than the threshold (~ 2 J cm^{-2}) usually lead to nanosecond laser ablation, so that the plasma is always created above the target surface. Plasma self-regulating absorption via inverse Bremsstrahlung (IB) is the reason for the laser ablation process. At higher laser irradiation, highly dense ionized plasma mediates the laser–target interactions. Via the IB process, free electrons absorb photons by which energy is gained from the laser beam during collisions with neutral and ionized atoms. Thus due to electron collisions with the excited and ground-state neutrals, vapor ionization and excitation take place. In the IR laser ablation process, vaporization creates primary electrons which have laser photon absorption ability at low electron density. Due to the high absorption of infrared radiation, its result is strong electron heating and breakdown ionization at very low laser intensities. On the other hand, in UV laser ablation, the photon energies are almost near the typical ionization energies of the excited atoms. Moreover, due to higher temperature of the electronic gas, plasma etching with UV irradiation might be possible. The higher density and temperature of the UV-induced plume lead to a large number of excited atoms, which could be photo-ionized by the several photon impacts. The presence of the highly excited fluorine ions in plume significantly increases the fragment combination rate to produce new clusters and molecules after UV photoablation. The effect of laser wavelengths causes different photoablation regimes, i.e., UV photoablation and plasma-induced ablation for excimer and Nd:YAG lasers, respectively.

IB is a wavelength-dependent effect proportional to λ^2; therefore it reduces four times using SHG of Nd:YAG at 532 nm with respect to the fundamental wavelength at 1064 nm. As a result, the contribution of IB becomes much weaker at shorter wavelengths of UV range, while the electron collisions in the plume notably contribute to the decomposition where the free electrons produced in the plume have gained energy in the electric field of the laser accordingly.

Fragment density diffused into the glass surface

Fluorine or fluorine content fragments can diffuse into glass surface so that we can write:

$$\frac{\partial N}{\partial t} = D \frac{\partial^2 N}{\partial x^2}, \quad (4)$$

where N, t, x and D are fragment density, time, depth of penetration and diffusivity, respectively. We suppose that fragment density in the glass surface before diffusion is negligible. The boundary conditions are at $x = x_0$, $N = N_0$ and at $x = \infty$, $N = 0$. The latter boundary condition is valid where there are not any fragments. The solution of (14) under those conditions is [6]:

$$N(x,t) = N_0 \mathrm{erfc} \frac{x}{2\sqrt{Dt}}. \quad (5)$$

The total number of fragments in unit area is:

$$Q(t) = \int_0^\infty N(x,t) \mathrm{d}x = \frac{2}{\sqrt{\pi}} \sqrt{Dt} N_0. \quad (6)$$

Then, we can estimate N_0 as:

$$N_0 = \frac{2Q(t)\sqrt{\pi}}{\sqrt{Dt}}. \quad (7)$$

Depth of penetration of fragments into a solid

We can use the following formula for approximating plasma fragments' penetration depth into glass surface [7]:

$$\frac{\mathrm{d}E}{\mathrm{d}x} = \frac{4\pi z^2 q^4 NZ \times (3 \times 10^9)^4}{Mv^2 \times 1.6 \times 10^{-6}} \left[\ln \frac{2Mv^2}{I} - \ln\left(1 - \frac{v^2}{c^2}\right) - \frac{v^2}{c^2}\right] \left(\frac{\mathrm{MeV}}{\mathrm{cm}}\right), \quad (8)$$

where z is the atomic number of ionized particles, M rthe est mass of ionized particles, v the velocity of ionized particles, N the number of absorber materials contained in unit volume, Z the atomic number of absorber material, c the velocity of light in vacuum and I the mean potential of ionization and excitation of absorber atoms ($I = 2.16 \times 10^{-11} Z$).

Results and discussion

Figure 3 shows the whole irradiated sample. Laser-irradiated regions are in the central part of the sample. There are four craters on the sample. The first two craters on top of the sample surface correspond to laser irradiation at 800 mbar SF_6 ambient gas and the next two craters concern laser shooting at vacuum condition. The lack of any crack on the sample after irradiation by Nd:YAG laser is a noticeable result.

The morphology of the irradiated samples was studied subsequently. Figure 4**a**–**c** illustrates the SEM micrograph of amorphous SiO_2 glass surface irradiated by 9 kJ/cm^2 of fundamental harmonic Nd:YAG laser dose at 800 mbar SF_6 pressure.

Figure 5**a**–**c** illustrates the SEM micrograph of amorphous SiO_2 glass surface irradiated by 9 kJ/cm^2 of fundamental harmonic Nd:YAG laser dose in vacuum.

A comparison between the two irradiated regions shows that in SF_6 atmosphere, we have more significant morphology changes due to laser irradiation. The difference could be visible even on the boundary region.

LIBS of SiO_2 glass in a typical SF_6 atmosphere (800 mbar) was performed using a focused laser beam at 1064 nm to investigate the SF_6 decomposed components. Figure 6 shows the emission characteristic lines due to significant fluorine radicals during laser irradiation. Excited fluorine F(I) characteristic lines at 634.850 and 690.247 nm are detectable. It indicates that SF_6 molecules are decomposed due to the energetic electrons and excited atoms such as the reactive oxygen. The reactive oxygen O(I) and O(II) lines were also detected due to SiO_2 dissociation after the ejection into gaseous SF_6 atmosphere to contribute further SF_6 decomposition.

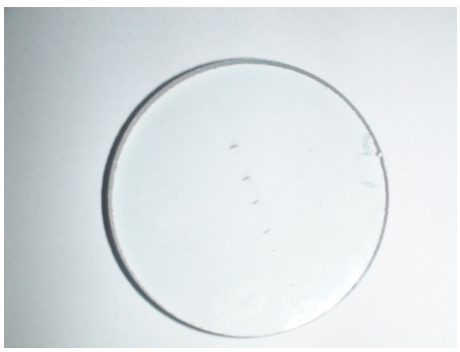

Fig. 3 Glass target after laser irradiation. The first two craters on top of the sample surface correspond to laser irradiation at 800 mbar SF_6 ambient gas and the next two craters correspond to laser shooting at vacuum condition

As mentioned in Eq. (3) due to linearity of that equation, we just need two points for obtaining the Boltzmann plot. The left-hand side of Eq. (3) versus E_i contains the slope of kT_e^{-1}. The coefficients A_{ij} and g_i are taken from the National Institute for Standards and Technology (NIST) atomic spectra database [8]. From F(I) lines in spectral region of 630– 695 nm, the plasma temperature was obtained as ~2000 K. This temperature is much lesser than the metallic or other gaseous materials' plasma temperatures. The main reason for this may be the more electronegativity of fluorine with respect to metallic or other materials. Considering the excitation energy of the level of F(I), comparison with a metallic ion shows that the fluorine ion excitation energy is nearly twice greater than that of the metallic ion. So, a noticeable part of the laser energy is spent in ionizing the fluorine atoms and the remaining part of this energy belongs to the plasma temperature. In the case of metallic or other materials, the ionizer portion of the laser energy is lower than that of fluorine, so the plasma temperature is higher than that of fluorine.

From data of our previous work [1] and Eq. (3), we have: $Q_{\mathrm{Nd:YAG}} = 320{,}000\ \mathrm{mm}^{-2}$, $Q_{\mathrm{SHG\ \ Nd:YAG}} = 370{,}000\ \mathrm{mm}^{-2}$ and $Q_{\mathrm{ArF}} = 34{,}000\ \mathrm{mm}^{-2}$. So we conclude: $N_{0,\mathrm{Nd:YAG}}/N_{0,\mathrm{ArF}} = 9.4$, $N_{0,\mathrm{Nd:YAG}}/N_{0,\mathrm{SHG\ \ Nd:YAG}} = 0.9$ and $N_{0,\mathrm{SHG\ Nd:YAG}}/N_{0,\mathrm{ArF}} = 10.9$. These results show that although N_0 (solid solubility) is not a linear function of temperature, we can conclude that the temperature of the irradiated area of glass surface in the Nd:YAG laser exposure is several times greater in comparison with ArF laser irradiation. In addition, the temperature of the irradiated glass surface in SHG of Nd:Yag exposure is slightly greater than in Nd:YAG laser irradiation. Those results showed in another manner the plasma-induced ablation and dissociation of SF_6 molecules near the glass surface in Nd:YAG laser irradiation as well as photoablation and SF_6 molecule decomposition near the glass surface in ArF laser exposure.

Using Eq. (8) and ignoring the terms which contain (v/c) ratio, considering the glass as the absorber material and F^- as the ionized particle and replacing their atomic number into the equation, we conclude that the penetration depth is very small (nearly zero) so that fluorine would be merely on the glass surface.

Conclusion

Glass surface modification occurred using Nd:YAG laser irradiation in SF_6 atmosphere. This kind of surface

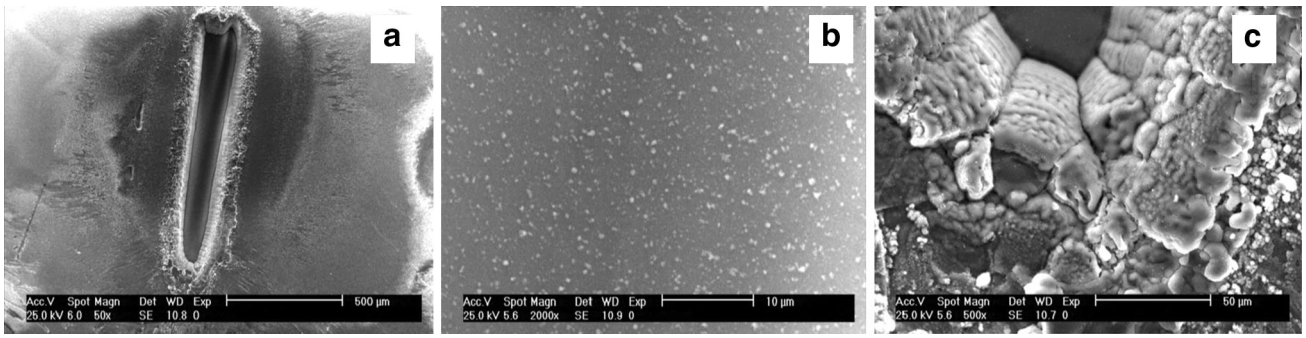

Fig. 4 **a** Crater created by laser irradiation on the glass target, **b** the crater's internal region surface morphology, **c** morphology of the crater boundary (fundamental harmonic of Nd:YAG laser, 9 kJ/cm^2, 800 mbar SF_6 atmosphere)

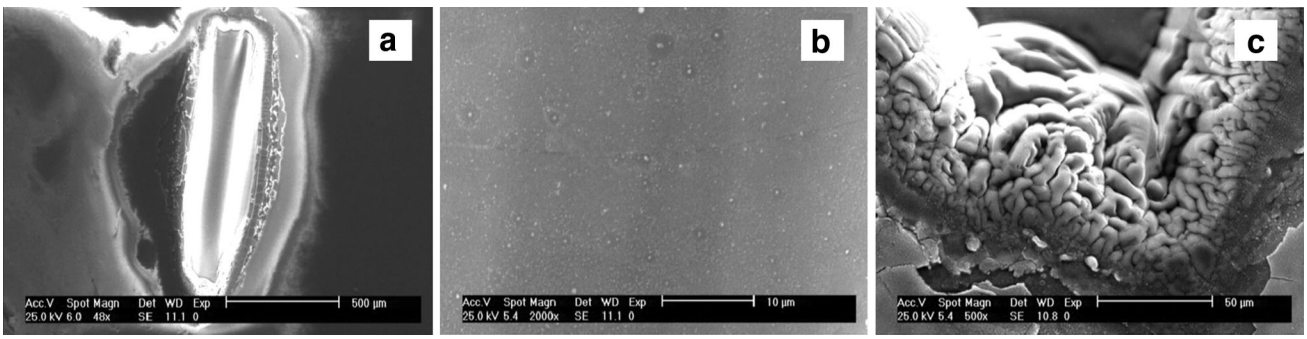

Fig. 5 **a** Crater created by laser irradiation on the glass target, **b** the crater's internal region surface morphology, **c** morphology of the crater boundary (fundamental harmonic of Nd:YAG laser, 9 kJ/cm^2, vacuum)

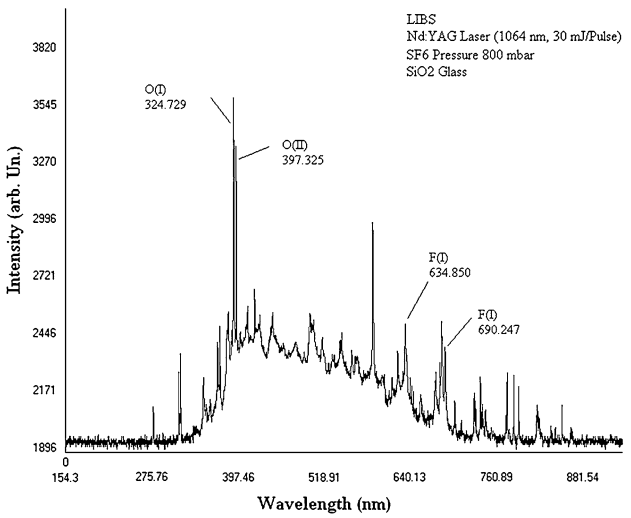

Fig. 6 Emission lines obtained by LIBS from amorphous SiO_2 glass surface within a cell filled with SF_6 at 800 mbar due to Nd:YAG laser exposure (10 ns, 1064 nm, 30 mJ/pulse)

modification embedded physical and chemical changes on the glass surface, which probably led to changes of the optical properties of irradiated glass. The laser irradiation on the SiO_2 glass surface in SF_6 ambient gas at 1064 nm wavelength was investigated. In fact, SF_6 decomposition by laser leads to the subsequent fluorine penetration into the SiO_2 layer. Laser breakdown spectroscopy (LIBS) shows that pulsed laser irradiation on SiO_2 surface in an SF_6 atmosphere induces gas decomposition. It produces the plasma containing reactive species to restructure the glass surface also. The plasma temperature creates at SF_6 atmosphere was lower than air ones. The main reason may be the more electronegativity of the fluorine comparison to other materials. The diffusion equation was used and it was shown that there were differences between irradiated zone temperatures at various laser wavelengths. Moreover, the use of penetration depth of ionized particle into a target showed that fluorine ions merely located on the glass surface and changed its surface chemical composition.

References

1. Dehghanpour, H.R., Parvin, P.: Jpn. J. Appl. Phys. **49**, 075803 (2010)

2. Sajad, B., Parvin, P., Bassam, M.A.: J. Phys. D: Appl. Phys. **37**, 3402 (2004)
3. Dehghanpour, H.R., Parvin, P.: Appl. Phys. B. **101**, 611 (2010)
4. Loper, G.L., Tabat, M.D.: Appl. Phys. Lett. **46**, 654 (1985)
5. Miziolek, A.W., Palleschi, V., Schechter, I.: Laser Breakdown Spectroscopy (LIBS) Fundamental and Applications. Cambridge University Press, New York (2006)
6. Hamilton, D.J., Howard, W.G.: Basic Integrated Circuit Engineering. McGraw-Hill, New York (1975)
7. Cember, H.: Introduction to Health Physics. Pergamon Press, USA (1983)
8. NIST electronic data base. http://physics.nist.gov/PhysRefData/ASD/Html/lineshelp.html